JACS
JOURNAL OF THE AMERICAN CHEMICAL SOCIETY

Communication

pubs.acs.org/JACS

Molecular Engineering of Potent Sensitizers for Very Efficient Light Harvesting in Thin-Film Solid-State Dye-Sensitized Solar Cells

Xiaoyu Zhang,[†,‡,∥] Yaoyao Xu,[†,∥] Fabrizio Giordano,[*,‡] Marcel Schreier,[*,‡] Norman Pellet,[‡] Yue Hu,[§] Chenyi Yi,[‡] Neil Robertson,[§] Jianli Hua,[*,†] Shaik M. Zakeeruddin,[*,‡] He Tian,[†] and Michael Grätzel[*,‡]

[†]Key Laboratory for Advanced Materials and Institute of Fine Chemicals, School of Chemistry and Molecular Engineering, East China University of Science and Technology, 130 Meilong Road, Shanghai 200237, China

[‡]Laboratoire de Photoniques et Interfaces, Institut des Sciences et Ingénierie Chimiques, École Polytechnique Fédérale de Lausanne, Station 6, 1015 Lausanne, Switzerland

[§]School of Chemistry, University of Edinburgh, King's Buildings, Edinburgh EH9 3FJ, U.K.

Supporting Information

ABSTRACT: Dye-sensitized solar cells (DSSCs) have shown significant potential for indoor and building-integrated photovoltaic applications. Herein we present three new D−A−π−A organic sensitizers, **XY1**, **XY2**, and **XY3**, that exhibit high molar extinction coefficients and a broad absorption range. Molecular modifications of these dyes, featuring a benzothiadiazole (BTZ) auxiliary acceptor, were achieved by introducing a thiophene heterocycle as well as by shifting the position of BTZ on the conjugated bridge. The ensuing high molar absorption coefficients enabled the fabrication of highly efficient thin-film solid-state DSSCs with only 1.3 μm mesoporous TiO_2 layer. **XY2** with a molar extinction coefficient of 6.66×10^4 M^{-1} cm^{-1} at 578 nm led to the best photovoltaic performance of 7.51%.

After 25 years of thorough study and development, dye-sensitized solar cells (DSSCs) are nowadays moving toward industrial production, aided by their simple and low-cost fabrication process, large range of colors, transparency, and high photovoltaic conversion efficiency (PCE), particularly under low-illumination conditions.[1,2] Solid-state DSSCs (ssDSSCs) employing hole-transporting materials (HTMs) have attracted significant interest as a practical solution for the problems posed by traditional liquid electrolytes.[3−5] In 1998, 2,2′,7,7′-tetrakis(*N*,*N*-di-*p*-methoxyphenylamine)-9,9′-spirobifluorene (spiro-OMeTAD) was reported as the first HTM for ssDSSCs. This material has since been widely used not only in ssDSSCs but also in perovskite solar cells.[4,6−8] A challenge for ssDSSC applications, however, remains the fact that spiro-OMeTAD only insufficiently infiltrates into thick mesoporous TiO_2 films. These films are therefore limited to a thickness of about 2−5 μm.[9,10] Thus, dyes with high extinction coefficients and broad absorption ranges are of great importance in order to achieve high solar-to-electricity conversion efficiencies on thin TiO_2 layers in ssDSSCs. Also, highly performing ssDSSCs, exibiting thin TiO_2 layers and strongly absorbing dyes, do not require scattering layers for optimal light harvesting. It is for this reason that they are very promising candidates for future applications in building-integrated photovoltaic (BIPV) windows and other areas, where aesthetics play an important role. Organic sensitizers are ideal candidates for thin-film cells because of their significantly higher molar extinction coefficients and lower cost compared to ruthenium-based sensitizers. Furthermore, their structural flexibility allows access to a larger parameter space for fine-tuning of dye properties.[11−13] This is particularly important in the case of dye regeneration and charge recombination processes at the TiO_2/dye/HTM interface, where molecular-level modifications of organic sensitizers are employed as an effective approach to impede undesirable charge recombination processes.[13−15] This is exemplified in the case of **Y123** (Figure 1) and **LEG4**, which feature bulky donors and

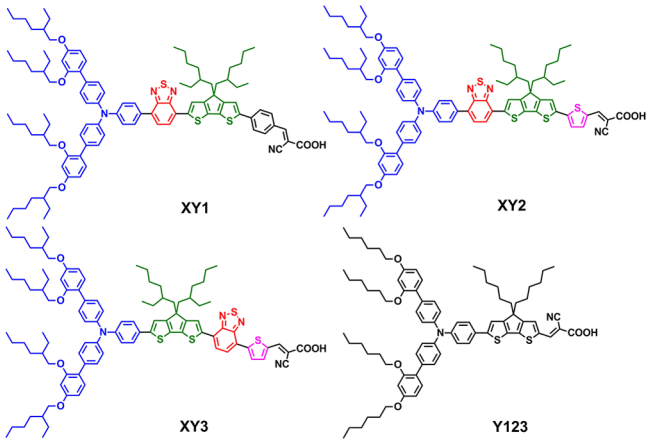

Figure 1. Molecular structures of **XY1**, **XY2**, **XY3**, and **Y123**.

cyclopentadithiophene (CPDT)-based π-bridges protected by alkoxy and alkyl chains, respectively. These bulky side chains shield the dye from the oxidized HTM and thereby inhibit recombination at the TiO_2/dye/HTM interface, leading to highly efficient ssDSSCs with spiro-OMeTAD.[16−18] For example, Burschka et al.[16] achieved a PCE of 7.2% from **Y123**-sensitized ssDSSCs using tris(2-(1*H*-pyrazol-1-yl)pyridine)-cobalt(III) (**FK102**) as a p-type HTM dopant (film thickness:

Received: May 23, 2016
Published: August 4, 2016

DOI: 10.1021/jacs.6b05281
J. Am. Chem. Soc. 2016, 138, 10742−10745

2.5 μm). Similarly, **LEG4**-sensitized ssDSSCs obtained PCEs of 7.7% with 1,1,2,2-tetracholoroethane-doped spiro-OMeTAD (film thickness: ~2.5 μm)[18] and 8.2% with copper phenanthroline as the hole conductor (film: ~6 μm transparent + 3 μm scattering layer).[19]

Previous work on DSSCs by our group as well as Zhu's group demonstrated that organic sensitizers with D−A−π−A structures outperform their D−π−A analogues because the introduction of an auxiliary acceptor (A) between the donor (D) and the π-bridge facilitates fine-tuning of the molecular energy levels. This leads to increased absorption and to an extension of the spectral response toward longer wavelengths.[13,20,21] From these works, benzothiadiazole (BTZ) emerged as a promising acceptor functionality.[20,22] Following these results, we here investigated three novel BTZ-based D−A−π−A sensitizers, **XY1**, **XY2**, and **XY3** (Figure 1). **XY1** showed a high molar extinction coefficient, which was further increased in **XY2** by introducing a heterocyclic thiophene unit onto the conjugated chain, also leading to an extension of the absorption toward the red. This effect was further enhanced upon exchanging the positions of BTZ and CPDT to obtain **XY3**, yielding a dye that absorbed up to the near-infrared region. The high molar extinction coefficients obtained from **XY1** and **XY2** enabled the fabrication of devices using very thin mesoporous TiO_2 layers (~1.3 μm) without compromising device performance.

The absorption spectra of **XY1**, **XY2**, **XY3**, and the reference dye **Y123** in CH_2Cl_2 are shown in Figure 2, and the parameters of

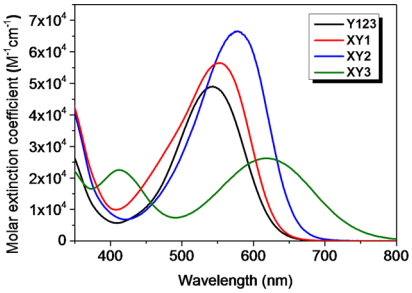

Figure 2. Absorption spectra of **Y123** (black), **XY1** (red), **XY2** (blue), and **XY3** (green) in CH_2Cl_2.

their optical and electrochemical properties are displayed in Table 1. The main absorption band can be assigned to intramolecular charge transfer (ICT) between the bulky donor and the cyanoacetic acid acceptor moiety.[13,23] From Figure 2, we can clearly see that **XY1** and **XY2** not only show bathochromic shifts of the low-energy absorption band but also increases in molar extinction coefficient compared with **Y123**. Among the investigated structures, **XY2** emerges as the most suitable sensitizer for ssDSSCs because of its high molar extinction coefficient of 6.66×10^4 M^{-1} cm^{-1} at its maximum absorption wavelength of 578 nm. Interestingly, by switching the positions of BTZ and CPDT (**XY3**), the absorption band was largely extended to the near-infrared region, red-shifting the low-energy absorption peak by 40 nm compared with **XY2**. However, the molar extinction coefficient of **XY3** drops to 2.62×10^4 M^{-1} cm^{-1}. At the same time, the HOMO energy level of **XY3** was upshifted to 0.75 V vs NHE, while **XY2** has its HOMO energy level at 0.91 V vs NHE, similar to those of **Y123** and **XY1**. Density functional theory (DFT) calculations revealed better overlap of the HOMO and LUMO in **XY2**, **XY1**, and **Y123** than in **XY3** (Figure S1), which provides a likely explanation for the higher molar extinction coefficients of **XY2**, **XY1**, and **Y123** compared with **XY3**.[24] From these data, it could also be noticed that CPDT contributes to electron donation in **XY3** (Figure S1), thereby shifting the HOMO energy level upward.

In order to test the performance of these dyes in an ssDSSC application, devices were prepared using spin-coated thin, transparent mesoporous TiO_2 layers. The resulting **XY2**-sensitized ssDSSC devices showed a reddish-purple color and substantial transparency of the light-absorbing layer, as shown in Figure 3a. The cross-sectional scanning electron microscopy

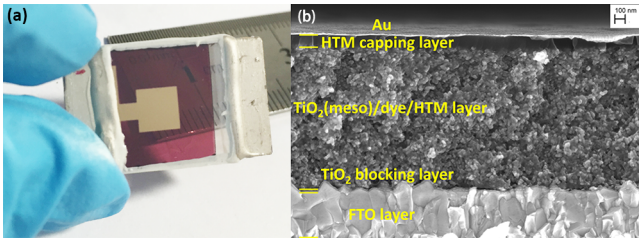

Figure 3. (a) Photograph and (b) cross-sectional SEM image of an ssDSSC device based on **XY2** with a ~1.3 μm thick transparent mesoporous TiO_2 layer.

(SEM) micrograph of the same device (Figure 3b) shows that spiro-OMeTAD penetrates the entire mesoporous structure while exhibiting a 100 nm capping layer on the surface, isolating the TiO_2 film from the Au counter electrode.

The photovoltaic performances of ssDSSCs based on **Y123**, **XY1**, **XY2**, and **XY3** under different light intensities are compiled in Table 2, and their corresponding current density−voltage (J−V) curves, dark-current plots, and incident photon-to-electron conversion efficiency (IPCE) spectra are displayed in Figure 4. The ssDSSCs with 1.3 μm TiO_2 films showed good reproducibility (Figure S3). **XY1** and **XY2** perform significantly better than **Y123** in ssDSSC devices because of their high molar extinction coefficients. The short-circuit current densities (J_{sc}) of ssDSSC devices with **XY1** and **XY2** reached over 10 mA cm^{-2}, which exceeds the value of 8.45 mA cm^{-2} observed from **Y123**. For devices based on the green dye **XY3**, a J_{sc} of 11.06 mA cm^{-2} was obtained but with a considerably lower open-circuit voltage (V_{oc}), losing over 100 mV compared with the other dyes. V_{oc} values of 0.798, 0.929, 0.942, and 0.904 V were obtained with **XY3**, **XY2**, **XY1** and **Y123**, respectively. Devices based on **XY2** and **XY1** led to good PCEs of 6.89% and 6.69%, respectively,

Table 1. Optical and Electrochemical Properties of XY1, XY2, XY3, and Y123

dye	λ_{max}[a]/nm ($\varepsilon/10^4$ M^{-1} cm^{-1})	E_{HOMO}[b]/ V vs NHE	E_{0-0}[c]/eV	E_{LUMO}[d]/ V vs NHE
Y123	543 (4.90)	0.92	2.01	−1.09
XY1	552 (5.65)	0.99	1.97	−0.98
XY2	578 (6.66)	0.91	1.92	−1.01
XY3	618 (2.62)	0.75	1.80	−1.05

[a]Absorption maximum in CH_2Cl_2 solution. [b]Measured in CH_2Cl_2 with 0.1 M tetra-*n*-butylammonium hexafluorophosphate as the electrolyte (working electrode, Pt; counter electrode, Pt wire; reference electrode, SCE; calibrated with ferrocene/ferrocenium as an external reference). [c]E_{0-0} was estimated from the absorption onset wavelength in the UV−vis absorption spectra of the dyes. [d]E_{LUMO} was estimated by subtracting E_{0-0} from E_{HOMO}.

DOI: 10.1021/jacs.6b05281
J. Am. Chem. Soc. 2016, 138, 10742−10745

Table 2. Performance Parameters of ssDSSCs Based on XY1, XY2, XY3, and Y123 under Different Light Intensities (I_0)

dye[a]	I_0/Sun	V_{oc}/V	J_{sc}/mA cm^{-2}	FF	PCE/%
Y123	96.6%	0.904	8.45	0.729	5.77
	49.9%	0.875	4.40	0.760	5.87
	9.3%	0.804	0.80	0.784	5.44
XY1	95.0%	0.942	10.02	0.674	6.69
	49.4%	0.907	5.31	0.717	6.98
	9.2%	0.815	0.95	0.767	6.46
XY2	95.5%	0.929	10.14	0.698	6.89
	50.1%	0.900	5.31	0.736	7.02
	9.2%	0.823	1.00	0.774	6.89
XY3	95.6%	0.798	11.06	0.596	5.50
	49.3%	0.774	5.67	0.656	5.85
	9.3%	0.703	0.98	0.683	5.06

[a]The bath composition is given in the Supporting Information.

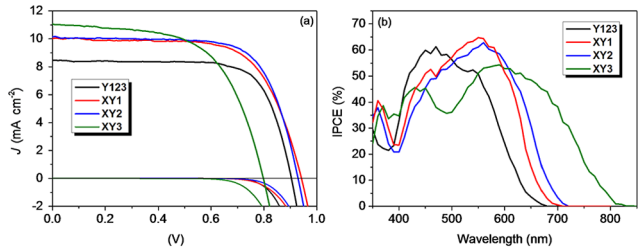

Figure 4. (a) J–V curves and dark currents of ssDSSCs with ~1.3 μm thick TiO_2 layers based on **Y123** (black), **XY1** (red), **XY2** (blue), and **XY3** (green) and (b) their corresponding IPCE plots under illumination of 10% Sun.

under 95% Sun illumination, which are considerably higher than that of devices based on the reference dye **Y123** (5.77%). A PCE of 5.50% was obtained for **XY3**, which is remarkable since its HOMO energy level is very close to that of spiro-OMeTAD, suggesting that the dye regeneration takes place despite the small driving force between the HOMO levels of the dye and HTM. The lower V_{oc} potentially indicates increased electron recombination at the TiO_2/dye/HTM interface. This effect will be further investigated below. PCEs under 50% and 10% light intensity were also measured, illustrating excellent potential for BIPV applications. Beyond 500 nm, devices based on **XY1** and **XY2** showed much higher IPCEs than those based on **Y123**. The peak IPCEs were found to be 71% at 560 nm with **XY1** and 70% at 580 nm with **XY2**, in contrast to 63% at 480 nm with **Y123**. In analogy to its absorption spectrum, devices based on **XY3** showed two absorption peaks with IPCEs of 60% at 590 nm and 50% at 430 nm, respectively. The photovoltaic performance of ssDSSCs based on these dyes was assessed as a function of film thickness, ranging from 0.25 to 2.0 μm (see sections 8 and 9 in the Supporting Information). Amazingly, with a TiO_2 film as thin as ~250 nm, ssDSSCs based on **XY2** and **XY1** reached PCEs of 4.34% and 4.01%, respectively.

The **XY2**-sensitized champion device achieved a PCE of 7.51%. This device also showed excellent PCEs under low light intensities (Table 3 and Figure 5). Under 50% Sun illumination, a high PCE of 7.64% was reached, which still amounted to 7.00% under 10% Sun. Current dynamics measurements of photocurrent versus light intensity are shown in Figure 5b. These measurements demonstrate a significant linearity between the photocurrent and light intensity, suggesting that the photo-

Table 3. Performance Parameters of the Champion ssDSSC Based on XY2 under Different Light Intensities (I_0)

I_0/Sun	V_{oc}/V	J_{sc}/mA cm^{-2}	FF	PCE/%
100.5%	0.902	10.96	0.764	7.51
51.7%	0.870	5.80	0.785	7.64
9.6%	0.799	1.05	0.803	7.00

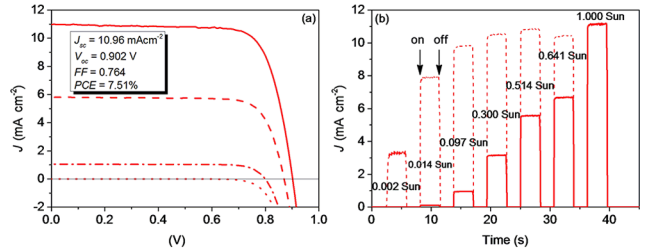

Figure 5. (a) J–V curves of the champion **XY2**-sensitized ssDSSC device under different light intensities (solid, 1 Sun; dashed, 0.5 Sun; dash-dot, 0.1 Sun; dotted, dark) and (b) the current dynamics (solid, measured data; dotted; integrated results under 1 Sun).

generated charges are efficiently evacuated in the investigated device.

In order to better understand the relationship between the molecular structure of the dye and the resulting device performance, we performed charge extraction and transient optoelectronic analyses. Two devices were measured for each dye. The voltage versus charge plot (Figure 6a) showed a weak

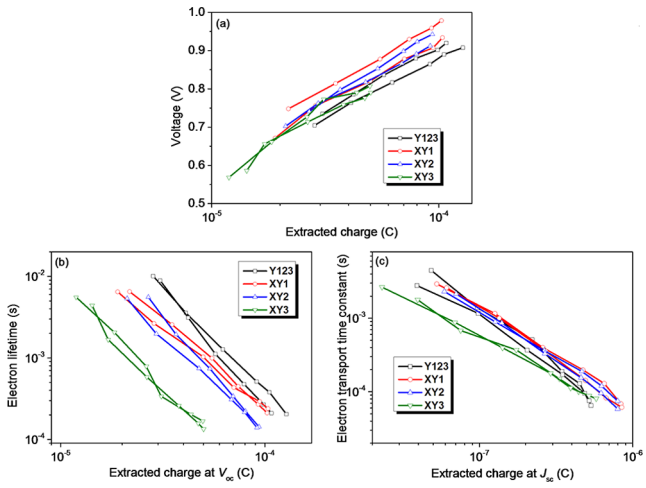

Figure 6. (a) Voltage and (b) electron lifetime vs extracted charge at V_{oc} and (c) electron transport time constant vs extracted charge at J_{sc} in ssDSSCs based on **Y123** (black), **XY1** (red), **XY2** (blue), and **XY3** (green).

upward shift of the electron quasi-Fermi level in TiO_2 for **XY1** and **XY2** compared with **Y123**. No shift was found for **XY3**. The higher V_{oc} of the devices employing **XY1** and **XY2** compared with **Y123** is in good agreement with these charge extraction measurements. The higher voltage is likely related to the more efficient photoconversion of the dyes with higher molar extinction coefficients. Moreover, the energetics of the TiO_2 conduction band are affected by the dipole generated by the surface-adsorbed dye, and a downward shift of the conduction band is expected to be directly proportional to the number of dye molecules covering the surface.[25] An increase in the molecular

DOI: 10.1021/jacs.6b05281
J. Am. Chem. Soc. 2016, 138, 10742–10745

size should result in a decreased dye loading on the TiO_2 surface,[26] which in turn would expose more bare TiO_2 surface to the spiro-OMeTAD, thus increasing the recombination rate. This reasoning is in agreement with the data on electron lifetimes shown in Figure 6b. For **XY1** and **XY2** the electron lifetime was found to be 3 to 2 times lower than for **Y123**, depending on the illumination conditions.

The lower V_{oc} of the devices employing **XY3** is directly related to the electron lifetime. From Figure 6b it becomes clear that the recombination is 10 times faster for **XY3** than for **Y123**. The higher recombination rate is thus responsible for the 100 mV difference in V_{oc} for these dyes. We suggest that the presence of an auxiliary acceptor close to the TiO_2 surface could play a role in accelerating the recombination rate in concomitance with its lower driving force for regeneration.[27] Interestingly, we observed slightly longer electron transport time constants for **XY1** and **XY2** compared with **Y123** and **XY3**, as shown in Figure 6c.

In conclusion, through rational molecular structure modifications, we designed and investigated three novel organic sensitizers, **XY1**, **XY2**, and **XY3**, among which **XY1** and **XY2** exhibit very high molar extinction coefficients and **XY3** shows a broad absorption range reaching the near-infrared region. By these modifications, we were able to achieve the best efficiency reported to date for D−A−π−A sensitizers in a ssDSSC application. With a TiO_2 film thickness of ∼1.3 μm, ssDSSCs based on **XY1** and **XY2** reached impressively high PCEs of 6.69% and 6.89%, which are much higher than for **Y123**. The champion device based on **XY2** achieved a PCE of 7.51%. Despite the small offset between the HOMO energy levels of **XY3** and spiro-OMeTAD, a PCE of 5.50% was achieved in the ssDSSC using this dye. However, **XY3** led to more charge recombination, which was attributed to the short electron lifetime and low driving force for dye regeneration, thus resulting in a low device V_{oc}.

■ ASSOCIATED CONTENT

Supporting Information

The Supporting Information is available free of charge on the ACS Publications website at DOI: 10.1021/jacs.6b05281.

Details of reagents, materials, instruments, and characterization; synthetic routes, procedures, and characterization data for all new compounds; methodology and results of DFT calculations; details of fabrication of ssDSSCs and photovoltaic and phototransient measurements; results of the reproducibility test; and photovoltaic performance of ssDSSCs with different film thicknesses (PDF)

■ AUTHOR INFORMATION

Corresponding Authors

*fabrizio.giordano@epfl.ch
*marcel.schreier@epfl.ch
*jlhua@ecust.edu.cn
*shaik.zakeer@epfl.ch
*michael.graetzel@epfl.ch

Author Contributions

‖X.Z. and Y.X. contributed equally.

Notes

The authors declare no competing financial interest.

■ ACKNOWLEDGMENTS

This work was supported by NSFC for Creative Research Groups (21421004), NSFC/China (21372082, 21572062, and 91233207), and the Programme of Introducing Talents of Discipline to Universities (B16017). X.Z. thanks the China Scholarship Council (CSC) for the financial support of a visiting program at EPFL. M.S. thanks Siemens AG for funding. M.G. acknowledges financial support from the Swiss National Science Foundation and CTI 17622.1 PFNM-NM, glass2energy sa (g2e), Villaz-St-Pierre, Switzerland.

■ REFERENCES

(1) O'Regan, B.; Grätzel, M. *Nature* **1991**, *353*, 737.
(2) Hagfeldt, A.; Boschloo, G.; Sun, L. C.; Kloo, L.; Pettersson, H. *Chem. Rev.* **2010**, *110*, 6595.
(3) Grätzel, M. *MRS Bull.* **2005**, *30*, 23.
(4) Yum, J.-H.; Chen, P.; Grätzel, M.; Nazeeruddin, M. K. *ChemSusChem* **2008**, *1*, 699.
(5) Vlachopoulos, N.; Zhang, J.; Hagfeldt, A. *Chimia* **2015**, *69*, 41.
(6) Bach, U.; Lupo, D.; Comte, P.; Moser, J. E.; Weissörtel, F.; Salbeck, J.; Spreitzer, H.; Grätzel, M. *Nature* **1998**, *395*, 583.
(7) Burschka, J.; Pellet, N.; Moon, S. J.; Humphry-Baker, R.; Gao, P.; Nazeeruddin, M. K.; Grätzel, M. *Nature* **2013**, *499*, 316.
(8) Bi, D.; Tress, W.; Dar, M. I.; Gao, P.; Luo, J.; Renevier, C.; Schenk, K.; Abate, A.; Giordano, F.; Baena, J.-P. C.; Decoppet, J.-D.; Zakeeruddin, S. M.; Nazeeruddin, M. K.; Grätzel, M.; Hagfeldt, A. *Sci. Adv.* **2016**, *2*, e1501170.
(9) Snaith, H. J.; Humphry-Baker, R.; Chen, P.; Cesar, I.; Zakeeruddin, S. M.; Grätzel, M. *Nanotechnology* **2008**, *19*, 424003.
(10) Ding, I.-K.; Tétreault, N.; Brillet, J.; Hardin, B. E.; Smith, E. H.; Rosenthal, S. J.; Sauvage, F.; Grätzel, M.; McGehee, M. D. *Adv. Funct. Mater.* **2009**, *19*, 2431.
(11) Mishra, A.; Fischer, M. K. R.; Bäuerle, P. *Angew. Chem., Int. Ed.* **2009**, *48*, 2474.
(12) Liang, M.; Chen, J. *Chem. Soc. Rev.* **2013**, *42*, 3453.
(13) Zhang, X.; Grätzel, M.; Hua, J. *Front. Optoelectron.* **2016**, *9*, 3.
(14) Lu, J.; Chang, Y.-C.; Cheng, H.-Y.; Wu, H.-P.; Cheng, Y.; Wang, M.; Diau, E. W.-G. *ChemSusChem* **2015**, *8*, 2529.
(15) Nguyen, W. H.; Bailie, C. D.; Burschka, J.; Moehl, T.; Grätzel, M.; McGehee, M. D.; Sellinger, A. *Chem. Mater.* **2013**, *25*, 1519.
(16) Burschka, J.; Dualeh, A.; Kessler, F.; Baranoff, E.; Cevey-Ha, N.-L.; Yi, C.; Nazeeruddin, M. K.; Grätzel, M. *J. Am. Chem. Soc.* **2011**, *133*, 18042.
(17) Xu, B.; Huang, J.; Ågren, H.; Kloo, L.; Hagfeldt, A.; Sun, L. *ChemSusChem* **2014**, *7*, 3252.
(18) Xu, B.; Gabrielsson, E.; Safdari, M.; Cheng, M.; Hua, Y.; Tian, H.; Gardner, J. M.; Kloo, L.; Sun, L. *Adv. Energy Mater.* **2015**, *5*, 1402340.
(19) Freitag, M.; Daniel, Q.; Pazoki, M.; Sveinbjörnsson, K.; Zhang, J.; Sun, L.; Hagfeldt, A.; Boschloo, G. *Energy Environ. Sci.* **2015**, *8*, 2634.
(20) Wu, Y.; Zhu, W. *Chem. Soc. Rev.* **2013**, *42*, 2039.
(21) Wu, Y.; Zhu, W.-H.; Zakeeruddin, S. M.; Grätzel, M. *ACS Appl. Mater. Interfaces* **2015**, *7*, 9307.
(22) Mathew, S.; Yella, A.; Gao, P.; Humphry-Baker, R.; Curchod, B. F. E.; Ashari-Astani, N.; Tavernelli, I.; Rothlisberger, U.; Nazeeruddin, M. K.; Grätzel, M. *Nat. Chem.* **2014**, *6*, 242.
(23) Zhang, X.; Mao, J.; Wang, D.; Li, X.; Yang, J.; Shen, Z.; Wu, W.; Li, J.; Ågren, H.; Hua, J. *ACS Appl. Mater. Interfaces* **2015**, *7*, 2760.
(24) Lee, Y.; Jo, A.; Park, S. B. *Angew. Chem., Int. Ed.* **2015**, *54*, 15689.
(25) Ronca, E.; Pastore, M.; Belpassi, L.; Tarantelli, F.; De Angelis, F. *Energy Environ. Sci.* **2013**, *6*, 183.
(26) Yang, J.; Ganesan, P.; Teuscher, J.; Moehl, T.; Kim, Y. J.; Yi, C.; Comte, P.; Pei, K.; Holcombe, T. W.; Nazeeruddin, M. K.; Hua, J.; Zakeeruddin, S. M.; Tian, H.; Grätzel, M. *J. Am. Chem. Soc.* **2014**, *136*, 5722.
(27) Haid, S.; Marszalek, M.; Mishra, A.; Wielopolski, M.; Teuscher, J.; Moser, J. E.; Humphry-Baker, R.; Zakeeruddin, S. M.; Grätzel, M.; Bäuerle, P. *Adv. Funct. Mater.* **2012**, *22*, 1291.

DOI: 10.1021/jacs.6b05281
J. Am. Chem. Soc. 2016, 138, 10742−10745